Glass Formation in $Fe_{50-x}Cr_{15}Mo_{14}C_{15}B_6M_x$ (M= Y, Gd and x= 0,2) Bulk Metallic Glasses

A. Bouchareb[1,2], R. Piccin[1], B. Bendjemil[1,2], M. Baricco[1]

[1]*Dipartimento di Chimica I.F.M/NIS/CNISM/INSTM, Università di Torino, Via P. Giuria 9, 10125 Torino Italy;* [2]*Laboratoire d'Etude et la Recherche de l'Etat Condensé - LEREC, University of Badji Mokhtar P. Box 12, 23000. Annaba, Algeria;* [3]*University of Guelma, P. Box 12, 24000, Guelma, Algeria*

Abstract

In the present work, the glass formation of $Fe_{50-x}Cr_{15}Mo_{14}C_{15}B_6M_x$ (x = 0,2 and M = Y,Gd) alloys has been investigated. Wedge shaped bulk samples, with thickness from 2 mm up to 5 mm, were prepared by copper mold casting technique. Ribbons of the same compositions, with 30 µm in thickness, were produced by melt-spinning technique. Thermal and structural properties were measured using High Temperature Differential Scanning Calorimetry and X-ray diffraction, respectively. The microstructure has been observed by Scanning Electron Microscopy and chemical composition was checked by Energy Dispersion Spectroscopy. In the case of ribbons, fully amorphous phase was observed for all compositions. Copper mold casting technique leads to a fully amorphous structure for bulk samples up to 2 mm only for composition containing Y or Gd. Such elements can act as oxygen scavengers, avoiding heterogeneous nucleation. The role of Y and Gd on glass formation is also discussed on the basis of the melting behavior.

Keywords: Bulk Metallic Glass; Glass Forming Ability; Thermal Stability.

1. Introduction

Metallic glasses have attracted much attention due to their fascinating properties, such as high strength and hardness, ultra-soft magnetic properties and good corrosion resistance [1,2]. However, high cooling rates around 10^5-10^6 K/s are required to obtain metallic glasses, which leads to limitation in size, at least in one dimension. Therefore, metallic glasses are usually obtained as thin films or as ribbons, with a thickness in the order of 10 µm. In the last decades, new bulk metallic glasses (BMG) were developed in Zr-, Ti-, Ni-, Pd-, Mg-, Fe-, Cu-based alloys [3], which can be obtained in an amorphous state in mm or cm-dimension, due to low critical cooling rates around 10^2-10^0 K/s.

Amorphous Fe-based alloys are known as amorphous steels [4]. They have a compressive strength much higher then the corresponding crystalline counterparts [5]. Therefore, this new class of materials shows strong potential applications in many technological fields. Moreover, recent developments allowed the preparation of amorphous steels from commercially pure elements [6], as well as from raw materials with low costs [7]. For instance, it has been reported that the

maximum diameter of Fe-based bulk glassy alloys, exhibiting high fracture strength of over 4000 MPa, is 5 mm for Fe–Co–B–Si–Nb system [5]. A maximum sample diameter up to 16 mm has been obtained by conventional copper mold casting method in amorphous steels with high glass forming ability (GFA) [4,8,9]. In order to improve the GFA, the minor alloying addition is a very important technique [5,10,11]. It was reported that the addition of suitable amounts of rare earths, such as Y, Gd, Dy, Ho, Er and Gd in the Fe-Cr-Mo-C-B alloys improves the GFA [8,12-14]. It has been suggested that the remarkable improvement of the GFA originates mainly from two important effects. The first is the intrinsic role of the minor alloying elements in destabilizing the competing crystalline phase and stabilizing the liquid phase [4,8,15,16]; the second is that alloying elements, such as Y or Gd, may also act as oxygen scavengers, leading to the suppression of heterogeneous nucleation and improving the GFA [10,17,18].

The present work aims to demonstrate that a significant increasing in the GFA of a Fe-Cr-Mo-C-B alloy is achieved with the addition of a suitable amount of Y or Gd. In fact, amorphous steels preparation is usually performed on a laboratory scale, in quite clean environments. For this reasons, in this work, bulk samples production has been carried out in a commercial casting machine, with significant oxygen contaminations. So, it may give significant contributions for an industrial production of this new structural alloys.

2. Experimental

Ingots of $Fe_{50-x}Cr_{15}Mo_{14}C_{15}B_6M_x$ (M = Y, Gd and x = 0,2) master alloys were prepared from commercial-grade materials by arc-melting furnace under Ar atmosphere. In order to study the effect the Y and Gd on GFA, the liquid alloys were quenched in a copper mold with a wedge shape having a maximum thickness of 14 mm and length 70 mm. Bulk samples preparation has been performed in a commercial casting machine used for the jewellery industry. It consists in an upper chamber, in which the induction coil and the crucible are placed, and a lower one, which contains the copper mold. Both chambers can be evacuated until 10^{-1} mbar and subsequently filled with pure Ar. After melting, a suitable overpressure in the upper chamber allows the casting of the liquid alloy in the copper mold. For comparison, ribbons of 5 mm width and about 30 µm thickness were prepared using a single-roller melt spinner at a wheel speed of 24 m/s. X-ray diffraction was performed to examine the structure of the as-quenched samples using Panalytical X'Pert and Philips PW1830 Bragg-Brentano diffractometers with Cu Kα (λ=1.5418 Å) and Co Kα (λ=1.7897 Å) radiations, respectively. All X-ray diffraction (XRD) patterns will be reported as a function of the wave vector $S = 4\pi sin(\theta)/\lambda$, where θ is the scattering angle. Scanning electron microscopy (SEM) investigations were performed using Leica Stereoscan 420 microscope. The samples were embedded into a resin and investigated surfaces were progressively rubbed with a sandpaper with mesh sizes of 600, 1000 and 2400, respectively. In order to distinguish the amorphous matrix from

the embedded crystalline phases, the samples surfaces were polished with diamond paste and chemical compositions were checked using Energy Dispersion Spectroscopy (EDS). Thermal analysis was performed by a Setaram high temperature differential scanning calorimeter (HT-DSC) at a heating rate of 0.17 K/s. The samples were placed in an alumina pan with some surrounding alumina powder, in order to prevent sticking to the crucible walls. The calorimetric cell was evacuated and purged several times before measuring under flowing He. Calibration of the instrument has been performed from the temperature and heat of fusion of pure metals (Al, Ag, Au, Fe, Cu, Ni).

3. Results and discussions

Fig. 1 shows the XRD patterns of $Fe_{50-x}Cr_{15}Mo_{14}C_{15}B_6M_x$ (x = 0,2 and M = Y,Gd) as-quenched alloys. Samples have been taken from the wedge with different thicknesses: part D (a) up to 2 mm; part C (b) up to 3 mm and part H (c) up to
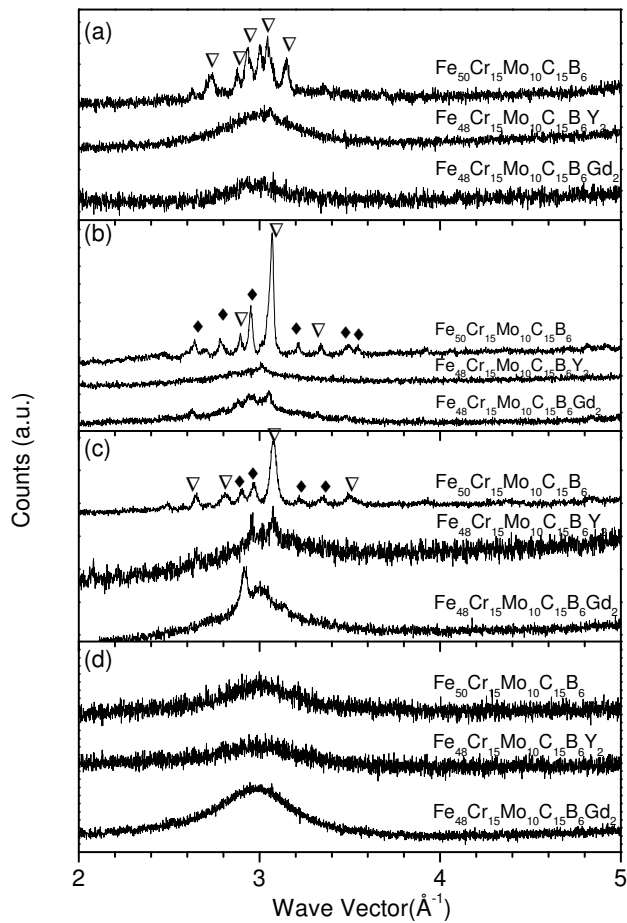

Fig. 1 XRD patterns of (a) down (D), (b) centre (C) and (c) high (H) parts of the wedge and (d) ribbons. Symbols correspond to $M_{23}C_6$ (∇), M_6C ($\blacklozenge$) type carbides.

5 mm, as schematically shown in Fig. 2. For comparison, patterns (d) are related to as-cast ribbons with thickness of about 30 µm. The results reveal that the addition of Y or Gd can significantly improve the GFA of the $Fe_{50-x}Cr_{15}Mo_{14}C_{15}B_6M_x$ (x = 0,2 and M = Y,Gd) alloys. In fact, the XRD patterns related to bulk samples, taken from H, C and D parts of the wedge, for the alloy without addition of Y or Gd reveal Bragg peaks corresponding to crystalline phases, namely $M_{23}C_6$ and M_6C type carbides. On the contrary, the XRD patterns of the samples taken from part D of the wedge, which have substituted 2 at.% of Fe by Y/Gd, show a broad diffraction halo, corresponding to a fully amorphous structure. In addition, the XRD patterns of samples with the same composition taken from H and C parts of the wedge, exhibit some sharp peaks superimposed to the amorphous halo, suggesting the presence of a partially amorphous structure. All XRD patterns of as-cast ribbons show only a broad halo, without crystalline peaks, indicating the presence of a fully amorphous structure.
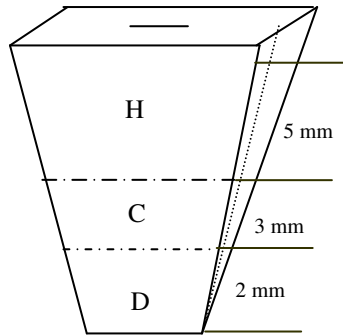

Fig. 2: Wedge shape of the copper mold used for casting, showing the considered parts taken in this study: H (high, 5 mm), C (center, 3 mm) and D (down, 2 mm).

The back scattered SEM images of the microstructures of the as-cast samples are shown in Fig. 3. Chemical analysis was obtained by EDS only for metals, because light elements can not be detected with accuracy. In as-cast sample without rare earth addition, taken from H part of the wedge (Fig. 3a), two crystalline phase can be observed. The phase corresponding to area I is enriched in Mo (49 at.%) with respect to the nominal composition, suggesting that it corresponds to M_6C-type carbide, formed as primary phase from the liquid during quenching. This phase is surrounded by an eutectic mixture, indicated as area II in the picture. It is composed by $M_{23}C_6$-type carbide, which contains a significant amount of Cr (17 at. %), and M_6C-type carbide. These observations are in good agreement with XRD results shown in Fig. 2. Crystalline phases could not be easily observed by SEM on the D part of the as-cast sample with the same composition (Fig. 3b). This may be due to a chemical composition of the phases close one to each other. In fact, the higher cooling rate obtained in the narrower section limited the nucleation and crystal growth, allowing the formation of a partially amorphous structure. In the case of the D parts of as-cast samples with Y or Gd addition, the electron back scattered SEM images (Figs. 3c and 3d) show an amorphous matrix with some

precipitates. EDS of light precipitate marked as I in Fig. 3c, gave a high Gd content (40 at.%) and, similarly, precipitates marked as I in Fig. 3d contains a high Y concentration (30 at.%). They appeared mainly at the surfaces of the sample, possibly due to rare earth oxidation generated during the casting.
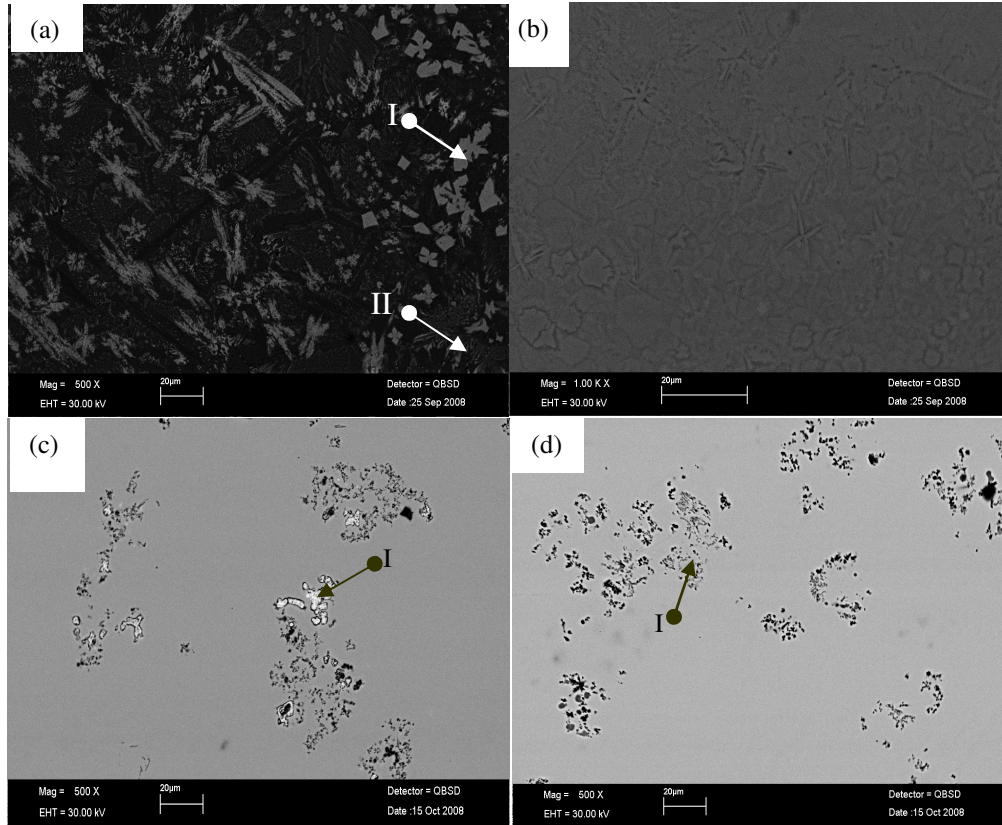

Fig.3: SEM back scattered electron images of: (a) H part and (b) D part of as-cast $Fe_{50}Cr_{15}Mo_{14}C_{15}B_6$; , (c) D part of as-cast $Fe_{48}Cr_{15}Mo_{14}C_{15}B_6Gd_2$ and (d) D part of as-cast $Fe_{48}Cr_{15}Mo_{14}C_{15}B_6Y_2$.

In order to gain further information on the effect Y or Gd addition on the GFA in amorphous steels, a HT-DSC analysis was performed to identify the thermal stability of the amorphous alloys and the corresponding melting behavior. The results are shown in Fig. 4 and the values of characteristic temperatures, indicated by arrows in Fig. 4, including glass transition temperature (T_g), crystallization temperature (T_x), supercooled liquid region temperature $\Delta T_x = T_x - T_g$, melting temperature (T_m) and liquidus temperature (T_l) are listed in table I. Fig. 4 shows the HT-DSC curves of crystallization of as-cast $Fe_{50-x}Cr_{15}Mo_{14}C_{15}B_6M_x$ (x = 0,2 and M=Y,Gd) BMGs taken from D parts of the wedge, together with those of as-cast ribbons. In all cases, three exothermic crystallization peaks were observed at about 600 °C, together with small exothermic signals at about 950 °C. It could be

observed that HT-DSC curves of bulk sample and as-cast ribbon with composition without Y or Gd addition show a clear difference in the crystallization peaks, due to the occurrence of a partial crystallization during casting of the bulk sample, which leaved an amorphous matrix with a composition different with respect to the nominal one. In the case of samples containing Y or Gd, the HT-DSC traces of crystallization appear very similar for ribbons and BMGs, confirming a the occurrence of a fully amorphization of the alloy during copper mold casting. It can be observed that T_x of $Fe_{50}Cr_{15}Mo_{14}C_{15}B_6$ amorphous alloy is higher with respect to other samples.

		$Fe_{50}Cr_{15}Mo_{14}C_{15}B_6$	$Fe_{48}Cr_{15}Mo_{14}C_{15}B_6Y_2$	$Fe_{48}Cr_{15}Mo_{14}C_{15}B_6Gd_2$
T_g(°C)	Ribbon	550	591	579
	Bulk	-	574	586
T_x(°C)	Ribbon	574	544	609
	Bulk	686	608	622
T_x-T_g(°C)	Ribbon	24	23	30
	Bulk	-	34	35
T_m (°C)	Ribbon	1117	1112	1119
	Bulk	1123	1118	1127
T_l(°C)	Ribbon	1203	1189	1188
	Bulk	1201	1192	1203

Table. 1: Thermal properties of as-cast bulk and ribbon amorphous steels obtained from HT-DSC analysis: T_g=glass transition temperature, T_x=crystallisation temperature, T_m= melting temperature, T_l=liquidus temperature.
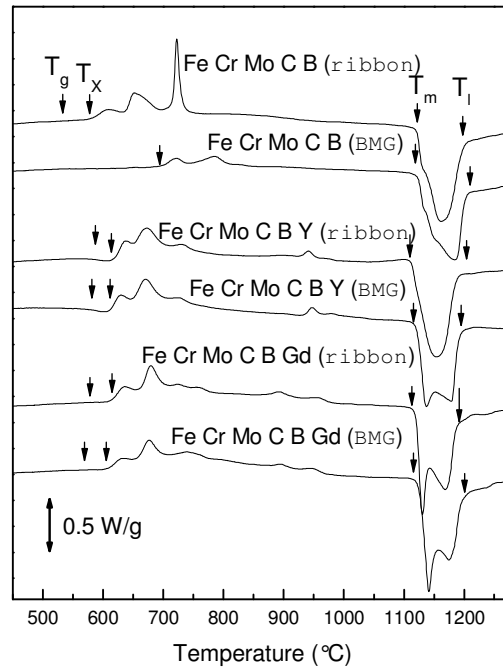

Fig. 4: HT-DSC curves of crystallization and melting for $Fe_{50-x}Cr_{15}Mo_{14}C_{15}B_6M_x$ (x = 0,2 and M = Y,Gd) as-cast bulk samples (D parts of the wedge) and ribbons.

HT-DSC traces for melting are also shown in Fig. 4. As reported previously [19], the first melting reaction corresponds to the disappearance of the eutectic mixture. The second endothermic signal is related to the melting of the M_6C-type carbide. The separation of the two melting reactions is less pronounced for samples without Y/Gd addition. At higher temperatures, a further liquidus signal may be observed for samples containing Gd, but it is less clear for the other samples. This results suggest that the melting behavior in the three samples is rather similar, even if small variations induced by the Y or Gd additions cannot be excluded.

The occurrence of a single amorphous phase in the bottom section of bulk samples with compositions containing Y or Gd is essentially due to a crystal nucleation suppression, or at least a nucleation that occurs at sufficiently low rate, associated to a limited growth. In addition, Y or Gd may act as an oxygen scavenger, reducing significantly the presence of heterogeneous nucleation sites. Moreover, the presence of rare earth in the alloy usually enhance the GFA of the alloy, due to its atomic size significantly larger than that of other element in the alloy [20], reducing the atomic diffusivity in the undercooled liquid. Besides, a liquid alloy which contains more than three elements can have a high packing density, due to the differences of atomic radii [21]. In the present case, the values for Y (2.27Å), Gd (2.54 Å), Mo (2.01 Å), Cr (1.85 Å), Fe (1.72 Å), B (1.17 Å), and C (0.91 Å) atoms lead to a stabilization of the amorphous phase when suitable compositions are selected. The similar values of thermal properties, reported in Table 1, suggest that the thermodynamic behavior of the liquid alloys has a limited effect on the GFA for the studied compositions.

4. Conclusions

The effect of addition of suitable amount of Gd and Y on the glass forming ability of $Fe_{50-x}Cr_{15}Mo_{14}C_{15}B_6M_x$ (M= Y, Gd and x= 0,2) alloys have been studied. Wedge shaped bulk ingots and ribbons were obtained by copper mold casting in an industrial machine and melt spinning techniques, respectively. Sample preparation conditions play an important role for amorphization. In fact, a fully amorphous structure has been obtained for all composition by rapid solidification. In the case of the bulk samples with $Fe_{50}Cr_{15}Mo_{14}C_{15}B_6$ composition, a partially amorphous structure was obtained only for the thinnest part of the ingot. On the contrary, the lower part of the bulk samples (about 2 mm thick) had a fully amorphous structure when a suitable amount of Y and Gd have been added. However, a partially amorphous structure was obtained in the central part of the ingots (about 3 mm thickness) with the same compositions. This paper demonstrates that the effect of Gd and Y additions to the amorphous steels are rather similar. In fact, both elements improves significantly the GFA of the amorphous steels prepared in a commercial casting machine with an oxygen contaminated environment.

References

[1] S. Sheng, C. Ma, S. Pang, T. Zhang, Glass forming ability and mechanical properties of Sm doped Fe-Cr-Mo-C-B glassy alloys, Mater. Trans. 46(12) (2005) 2949-2553

[2] A. Takeuchi, A. Inoue, Size dependence of soft to hard magnetic transition in (Nd, Pr)–Fe–Al bulk amorphous alloys, Mater. Sci. & Eng. 375(377) (2004) 1140–1144

[3] A. Inoue, A. Takeuchi, High strength bulk amorphous alloys, Mater. Trans. JIM 43(8) (2002) 1892-1906

[4] Z. P. Lu, C, T. Liu, J. R. Thompson, W. D. Porter, Structural amorphous steels, Phys. Rev. Lett. 92 (24) (2004) 245503-245507

[5] A. Inoue, B.L. Shen, C.T. Chang, Super-high strength of over 4000 MPa. for Fe-based bulk glassy alloys in $[(Fe_{1-x}Co_x)_{0.75}B_{0.2}Si_{0.05}]_{96}Nb_4$ system, Acta. Materiala 52(14) (2004) 4093–4099

[6] R. Hasegawa, Present status of amorphous soft magnetic alloys, J. Magn. Mater. 215-216(1) (2000) 240-245

[7] K. Hashimoto, K. Osada, T. Masumoto, S. Shimodaira, Characteristics of passivity of extremely corrosion-resistant amorphous iron alloys, Corros. Sci. 16(2) (1976) 71-76

[8] V. Ponnambalam, S. J. Poon, G. J. Shiflet, Fe-based metallic glasses with diameter thickness larger than one centimeter, J. Mater. Res. 19(5) (2004) 1320-1323

[9] J. Shen, Q. J. Chen, J. F. Sun, H. B. Fan, G. Wang, Exceptionally high glass-forming ability of an FeCoCrMoCBY alloy, Appl. Phys. Lett. 86(15) (2005) 151907-1-151907-3

[10] Z. P. Lu, C. T. Liu, W. D. Porter, Role of yttrium in glass formation of Fe-based bulk metallic glasses, Appl. Phys. Lett.83(13) (2003) 2581-2583

[11] V. Ponnambalam, S. Joseph Poon, G. Shiflet, Fe-Mn-Cr-Mo-(Y,Ln)-C-B (Ln=Lanthanides) bulk metallic glasses as formable amorphous steel alloys, J. Mater. Res. 19(10) (2004) 3046-3052

[12] M. Iqbal, J. I. Akhter, H. F. Zhang, Z. Q. Hu, Synthesis and characterization of bulk amorphous steels, J. of Non-Cryst. Solids 354(28) (2008) 3284-3290

[13] Tanya Aycan Baser, Marcello Baricco, Fe-based bulk metallic glasses with Y addition, J. of All. Comp. 190(8) (2006) 14569-14573

[14] Q. Chen, D. Zhang, J. Shen, H. Fan, J. Sun, Effect of yttrium on the glass forming ability of Fe-Cr-Mo-C-B bulk amorphous alloys, J. of All. Comp. 427 (1-2) (2007) 190–193

[15] A. Inoue, Stabilization of metallic supercooled liquid and bulk amorphous alloys, Acta. Materialia. 48(1) (2000) 279-306

[16] Z. P. Lu, C. T. Liu, C. A. Carmichael, W. D. Porter, Bulk glass formation in an Fe-based Fe–Y–Zr–M (M = Cr, Co, Al)–Mo–B system**,** J. Mater. Res. 19(3) (2004) 921-929.

[17] C. T. Liu, M. F. Chisholm, M. K. Miller, Oxygen impurity and microalloying effect in a Zr-based bulk metallic glass alloy, Intermetallics 10(11) (2002) 1105-1112

[18] Y. Zhang, M. X. Pan, D. Q. Zhao, R. J. Wang, W, H. Wang, Formation of Zr-based bulk metallic glasses from low purity of materials by yttrium addition, Mater. Trans. JIM 41(11) (2000) 1410-1414

[19] T.A. Baser, M. Bostrom, M. Stoica, A.R. Yavari, M. Baricco, Analysis of Melting and Solidification Behaviour of Glass-forming Alloys by Synchrotron Radiation, Adv. Eng. Mater. 9(6) (2007) 492-495

[20] Z.P. Lu, C.T. Liu, Role of minor alloying additions in formation of bulk metallic glasses: A Review, J. Mater. Science 39 (2004) 3965- 3974

[21] D.B. Miracle, A structural model for metallic glasses, Nature Mater. 3 (2004) 697-702